

## ERS-1 and CCRS C-SAR Data Integration for Look Direction Bias Correction using Wavelet Transform

J.S. Won\* \*\*\*\*, Wooil M. Moon\*, Vern Singhroy\*\* and Paul D. Lowman Jr.\*\*\*

\* The University of Manitoba, Winnipeg, Canada R3T 2N2

\*\* Canada Centre for Remote Sensing, Ottawa, Canada K1A 0Y7

\*\*\* Geophysics Branch, Code 921, Goddard Space Flight Center,  
Maryland 20771 U.S.A.(August 1994)

\*\*\*\* Present Address: Geophysics Team, Korea Ocean Research  
and Development Institute, P.O. Box 29, Ansan, Korea

### Summary

Look direction bias in a single look SAR image can often be misinterpreted in the geological application of radar data. This paper investigates digital processing techniques for SAR image data integration and compensation of the SAR data look direction bias. The two important approaches for reducing look direction bias and integration of multiple SAR data sets are (1) principal component analysis (PCA), and (2) wavelet transform (WT) integration techniques. These two methods were investigated and tested with the ERS-1 (VV - polarization) and CCRS\*s airborne (HH - polarization) C-SAR image data sets recorded over the Sudbury test site, Canada.

The PCA technique has been very effective for integration of more than two layers of digital image data. When there are only two sets of SAR data available, the PCA technique requires at least one more set of auxiliary data for proper rendition of the fine surface features. The WT processing approach of SAR data integration utilizes the property which decomposes images into approximated image (low frequencies) characterizing the spatially large and relatively distinct structures, and detailed image (high frequencies) in which the information on detailed fine structures are preserved. The test results with the ERS-1 and CCRS\*s C-SAR data indicate that the new WT approach is more efficient and robust in enhancing the fine details of the multiple SAR images than the PCA approach.

Key words: ERS-1 SAR, wavelet transform(WT), SAR image integration, look direction bias.

## Introduction

Although the importance of look direction for geologic applications of imaging radar has been recognized for some time (Ford, 1980), experience with airborne and orbital radar of the Canadian Shield has shown look direction to be not only important but dominant for geological structure rendition (Harris, 1984; Lowman et al., 1987; Singhroy, 1992; Singhroy et al., 1993). For a low relief terrain of uniform roughness and dielectric properties, typified by much of the Shield, topographic features within 20 degrees of parallelism with the look may be totally invisible. The reason is essentially that the local incidence angle for adjacent features, such as a ridge and valley, will be nearly identical. Backscatter will therefore be the same, and the topographic feature will not show up, unless of course there are associated features with different backscatter properties, such as a stream or lake.

The significance of this look direction bias is that for terrain like that of the Canadian Shield, including the Sudbury test site, roughly half the structure will in principle be invisible unless at least two look directions, preferably orthogonal, are acquired. Since this is not always possible, due to orbital constraints, it is necessary to take all feasible measures to compensate for look direction bias.

Integration methods for multiple layers of SAR data investigated and tested in this paper include : (1) the principal component analysis (PCA), and (2) the wavelet transform (WT) processing approach. The test data sets include the CCRS\*s airborne C-band SAR (HH - polarization) and the ERS-1 SAR (VV - polarization) data recorded over the Sudbury test site in Ontario, Canada.

The principal component analysis (PCA) is a well known technique often used for merging two or more remote sensing data sets (Kaneko, 1978; Byrne et al., 1980; Masuoka et al., 1987) for wide ranging application objectives. The first principal component image is normally dominated by detailed surface features highly correlated in all original input images. When the PCA technique was directly applied to two original test SAR data sets, significant loss of detailed surface structures in the integrated image occurred due to very low correlation between the test SAR data sets. In this particular case, it was apparent that at least one more auxiliary data set was required. A data set obtained through directional derivative was used as an auxiliary data, and the PCA processing with this additional data set has resulted in a relatively satisfactory integrated image.

The wavelet transform was first introduced by Morlet et al. (1982), which was then followed by rigorous theoretical developments (Grossman and Morlet, 1984; Meyer, 1986;

Daubechies et al., 1986; Daubechies, 1988; Daubechies, 1990; Mallat, 1989). Application fields of the wavelet transform are numerous today including signal analysis, music synthesis, computer vision analysis, compact image coding etc. The basic idea of the wavelet transform is decomposition of a signal function by projecting it on to the contracted (high frequency) and dilated (low frequency) versions of a selected wavelet. One can achieve multi-resolution signal analysis through the wavelet transform. The WT processing can in general be applied to any two dimensional digital data set. Miao and Moon (1993) have successfully applied the WT technique for improving S/N ratio of prestack seismic reflection data as well as for increasing the image resolution of the post-stack seismic data. The integration experiment discussed below mainly concerned merging two or more SAR data sets with the objective of reducing look direction bias. The WT processing approach of integrating SAR data utilizes only the approximated (low frequencies) image layer whereas the detailed image information of each original image remained unchanged. In this approach one can preserve the small minute details of the original higher resolution image while large structural features such as lineaments are properly merged and enhanced. The test results show that enhancement of lineaments using the WT technique is comparable or better than many other conventional approaches and the method itself is more robust than the PCA technique.

## Methodology

The basic principles of both PCA and WT have been well known and widely used in various disciplines of the digital image processing research. In this section only the relevant facts and some fundamental principles will be briefly reviewed and discussed.

**Principal Component Analysis (PCA)** : The PCA, also referred as Kahunen-Loeve transform, is a very versatile and well known technique for compression of dimensionality of highly correlated multi-spectral data (Kaneko, 1978; Byrne et al., 1980). Moon et al. (1991) tested the PCA approach for integrated geological study using SPOT data and airborne C-band SAR and reported that PCA can be an effective tool for delineating surface geological feature classification. Masuoka et al. (1987) carried out a similar PCA study with three sets of SAR data and demonstrated that the first principal component reconstruction produced a fairly detailed image of surface roughness.

**Wavelet Transform** : The wavelet transform is a mathematical tool for the time frequency or phase-space analysis of signals with multiple scales in resolution (Daubechies, 1990). Theoretical details of the wavelet transform are referred to papers listed in the references (Morlet et al., 1982; Grossman and Morlet, 1984; Meyer, 1986; Daubechies, et al., 1986; Daubechies, 1988; Daubechies, 1990). The central idea of the wavelet transform is decomposition of the signal function by projecting it to a sequence of contracted (high frequencies) and dilated (low frequencies) version of a selected wavelet.

The wavelet transform of a signal  $s(x)$  is given by

$$S(a, b) = \frac{1}{\sqrt{a}} \int s(x) h\left(\frac{x-b}{a}\right) dx \quad (1)$$

where the parameter  $a$  represents dilation and  $b$  represents the translation of the analyzing wavelet,  $s(x)$  is the input signal function which is to be transformed, and  $h^{(a,b)}(x)$  is an analyzing wavelet satisfying square integrability, i.e.

$$\int \frac{|H(k)|^2}{|k|} dk < \infty \quad (2)$$

where  $H(k)$  denotes the Fourier transform of  $h(x)$ . Here,  $x$  and  $k$  are the integration variables in the space and wavenumber domains respectively. The original signal function  $s(x)$  can then be reconstructed from  $S(a,b)$  through

$$s(x) = \frac{1}{C_g} \int \int \frac{1}{\sqrt{a}} h\left(\frac{x-a}{a}\right) \frac{1}{a^2} da db \quad (3)$$

where  $C_g = \int |g(x)|^2 dx$ . Mallat's algorithm was adopted in this research for the wavelet transform of SAR image data (Mallat, 1989).

Among numerous applications of the wavelet transform, multi-resolution decomposition of image(Mallat, 1989) provides the most suitable tool for the digital SAR image merging. Given a sequence of increasing resolutions, details of an image at a certain level of resolution can be defined as the difference of information between its approximation at that resolution and its approximation at the next lower level(Mallat, 1989). At a coarse resolution, the approximated image characterizes the larger and relatively distinct surface geological structures. A sequence of resolution levels and corresponding approximated images can then be reassembled to enhance certain look directions or a selected surface geological features.

ERS-1 and CCRS C-SAR Data Integration for Look Direction - Won et al.

Table 1. Parameters of the ERS-1 and the CCRS\*s airborne C-band SAR data used in this study.

	<b>Airborne SAR</b>	<b>ERS-1 SAR</b>
<i>Frequency</i>	C-band	C-band
<i>Polarization</i>	HH	VV
<i>Nominal Height</i>	6km	785km
<i>Flight or Orbit Direction</i>	app. 70° NE	app. 20° SW
<i>Look Direction</i>	look right	look right
<i>Resolution</i>	25 x 25m	30 x 30m



Figure 1. The CCRS\*s airborne C-band SAR image over the Sudbury test site, Canada.

## Test SAR Data

Two SAR data sets chosen for this research : (a) the ERS-1 C-band SAR (VV - polarization) data ; and (b) CCRS\*s airborne C-band SAR (HH - polarization) data are both C-band but the polarization of the imaging signal and the depression angles are quite different. The data acquisition parameters and data characteristics are listed in Table 1. The airborne C-band SAR data (Figure 1) were co-registered with the ERS-1 SAR data (Figure 2). The aircraft flight direction and the orbit track direction of the two data sets are nearly normal as listed in Table 1 and the look direction bias of each data set is also approximately at right angles.

The CCRS\*s airborne SAR image (Figures 1) provides in general better rendition of small detailed surface features than the higher altitude ERS-1 SAR image (Figure 2). The ERS-1 SAR image has poorer geologic rendition except the north to north-west trending linear features in the North Range which are highlighted, whereas the north to north-west



Figure 2. The ERS-1 SAR image over the Sudbury test site, Canada.

trending linear features are not clearly visible in the airborne SAR image due to the near EW flight direction (Singhroy et al., 1993). These features can be confirmed by Radon transform analysis as shown in Figure 3(a) (Won, 1992). Lack of north trending lineaments at the slope of  $-16^\circ$  in the airborne SAR data (dot dashed line in Figure 3(a)) is evident in the Radon transform amplitude plot. On the other hand, the ERS-1 SAR image (solid line in Figure 3(a)) has Radon transform amplitude peak at  $-26^\circ$ , which corresponds to the highlighted surface structural features including mostly north to north-west trending lineaments. The processing experiment in this paper was carried out to enhance the north to north-west trending lineaments of the ERS-1 image in the North Range of Sudbury, while retaining the detailed small scale geological renditions of the airborne SAR image.

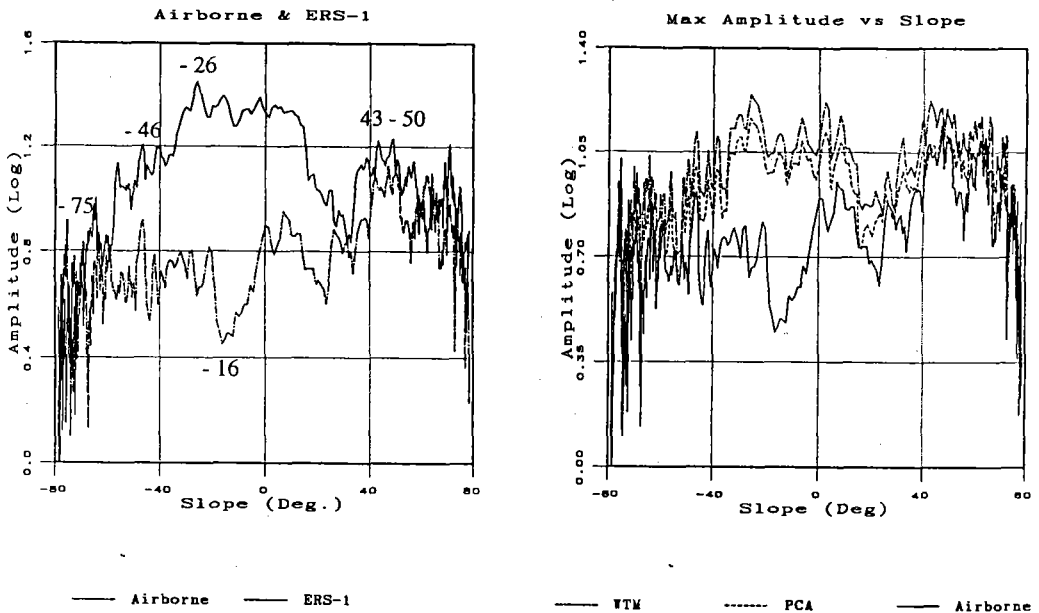


Figure 3. Maximum amplitude of the Radon transform versus slope: (a) solid line represents the Radon transform for the ERS-1 SAR data; (b) solid line is the original airborne SAR data, dashed line is the PCA processed result, and dot-dashed line is the wavelet transform processed result.

Table 2. Correlation coefficient of three data sets: the CCRS\*s airborne SAR data(Band 1), the ERS-1 SAR data(Band 2), and the lineament enhanced data(Band 3).

Band	1	2	3
1	1.00	-	-
2	0.16	1.00	-
3	0.74	0.4	1.00

### Integration Processing And Enhancing Of Features

**SAR Data Integration using PCA** : The first principal component image is generally dominated by highly correlated features from all input images. The correlation coefficient between the two test SAR data sets is, however, very low (0.16 in Table 2). Direct application of PCA using two original SAR data sets has resulted in significant loss of small scale structural details as shown in Figure 4.

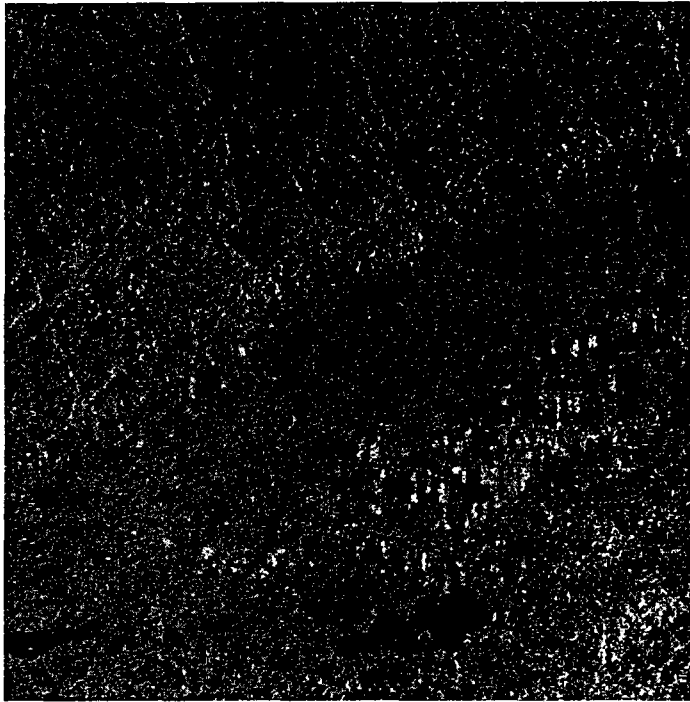


Figure 4. The PCA first component image of the ERS-1 and CCRS\*s C-band SAR image.



For proper reconstruction of a PCA processed image, at least one more auxiliary data layer is thus desirable. Lineament enhanced image using a directional derivative method (Haralick, 1984) was tested as an additional auxiliary data in this experiment. Correlation statistics of the three data sets are given in Table 2. The PCA first component image obtained using three data sets is shown in Figure 5. Compared to Figure 4, rendition of small geologic structures are considerably improved in Figure 5. Lineament enhancement in the resulting PCA image is confirmed by Radon Transform analysis (Figure 3(b)). The Radon transform amplitude low at or near the azimuth of  $-16^\circ$  for the airborne SAR data (solid line in Figure 3(b)) is now brought up in the PCA processed image (dashed line in Figure 3(b)).

In summary, the PCA approach is an effective way for integrating multiple SAR data sets and for compensating the look direction bias in each single SAR image.

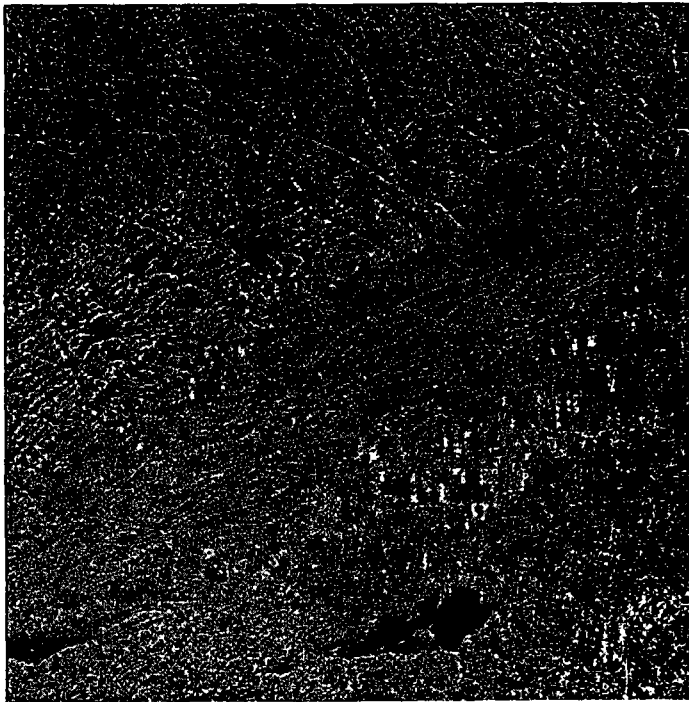


Figure 5. The PCA first component image of the ERS-1, airborne CCRS SAR image data and the auxiliary data (please see text).

**Wavelet Transform Processing and Integration** : The airborne SAR image (Figure 1) was decomposed into four quadratures using the WT analysis as shown in Figure 6. In this step, the first octave wavelet transform was carried out. Upper left quadrature in Figure 6 is an approximated image (low frequencies) at 1/2 resolution. The other three quadratures consist of detailed images (high frequencies) : upper right corresponds to horizontal high frequencies and vertical low frequencies of the original image; bottom left the horizontal low frequencies and vertical high frequencies; bottom right the high frequencies in both horizontal and vertical dimensions. As the octave of the wavelet transform increases, the upper left quadrature is decomposed in hierarchical structure.

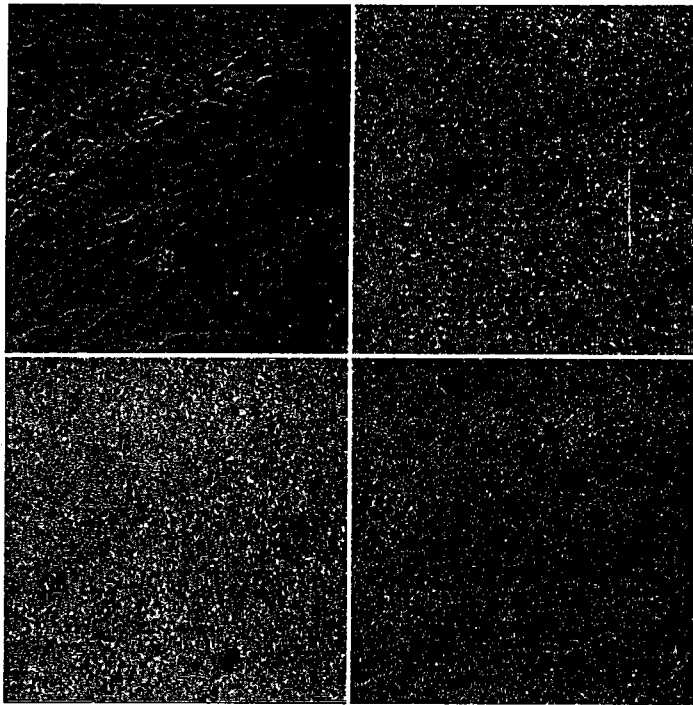


Figure 6. The wavelet transform of the CCRS\*s airborne SAR data: Upper left quadrature is approximated (low frequency) image at 1/2 resolution; upper right corresponds to horizontal high frequency and vertical low frequency decomposition of the original data; bottom left is the horizontal low frequency and vertical high frequency decomposition; and bottom right the high frequency in both horizontal and vertical dimensions.

Although the main objective of this integration experiment is enhancement of north to north-west trending lineaments in the airborne SAR image by merging the ERS-1 SAR data, detailed fine structures of the airborne SAR image must also be retained as much as possible. The approximated image of the wavelet transform characterizes the large scale structures, whereas the information on finer structures are retained throughout the wavelet transform processing. The actual merging process is limited only to the approximated image of the airborne and the ERS-1 SAR data. They were simple added after application of the wavelet transform of the first-octave. The new integrated and lineament enhanced image obtained by applying the wavelet transform is shown in Figure 7.

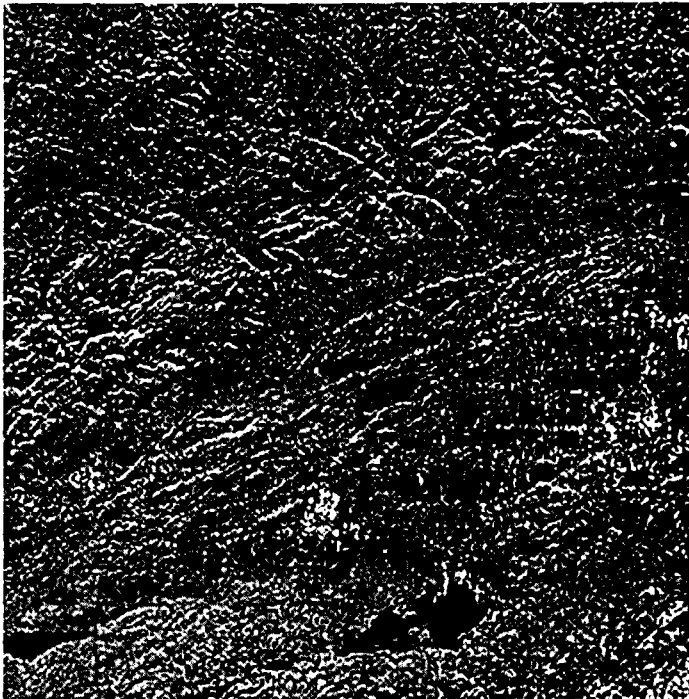


Figure 7. The wavelet transform processed integrated image of the ERS-1 and CCRS\*s airborne C-band SAR image.

The Radon transform analysis was carried with the results and compared with previous results. The result is shown in Figure 3(b) (dot-dash line). The Radon transform analysis plot (Figure 3(b)) shows overall improved enhancement of the lineaments in all directions. Enhancement of the finer surface features and the reduction of look direction bias in the ERS-1 SAR image were achieved without sacrificing the fine details of the airborne SAR data. In the PCA approach each pixel value of the merged image are rotated according to the eigenvalues chosen and it becomes impossible to retain original image characteristics. In this respect, the wavelet transform approach of processing, merging, and enhancing of look direction bias error appears superior when there are two or more sets of SAR data available.

## Conclusion

The PCA techniques has been very effective in integrating multiple layers of digital image data, including the SAR data. When the number of digital image layer is less than three, an additional set of auxiliary information is needed for proper image merging using the PCA technique.

The WT approach of processing and merging of multiple layers of SAR data is comparable or superior to the PCA approach while it preserves all the finer details in the higher resolution data layer. If one of the objectives of image integration includes preservation of finer resolution (high frequency) information, the WT approach provides a superior processing tool. The test results with the ERS-1 and CCRS\*s SAR image data sets over Sudbury, Canada, have demonstrated that slightly low resolution and considerably high depression angle ERS-1 data can be enhanced using high resolution low depression angle airborne SAR data for critical details on surface.

## Acknowledgement

This research is funded by an NSERC operating grant # A-7400 to W.M. Moon. The ERS-1 and CCRS\*s SAR image data were provided as a part of the Canadian ERS-1 scientific verification program.

## References

- Byrne, G.F., Crapper, P.F., and Mayo, K.K., 1980, Monitoring land-cover change by principal component analysis of multi-temporal Landsat data, *Remote Sensing of Environment*, 1, 887-888.
- Daubechies, I., Grossman, A., Meyer, Y., 1986, Painless non-orthogonal expansions, *J. Math. Phys.*, 27, 1271-1283.
- Daubechies, I., 1988, Orthogonal bases of compactly supported wavelets, *Comm. Pure Appl. Math.*, 41, 909-996.
- Daubechies, I., 1990, The wavelet transform, time-frequency localization and signal analysis, *IEEE Trans. Inform. Theory*, 36, 961-1005.
- Ford, J. P., 1980, Seasat orbital radar imagery for geological mapping: Tennessee Kentucky - Virginia, *American Association of Petroleum Geologists Bulletin*, 64, 2064-2094.
- Grossman, A., and Morlet, J., 1984, Decomposition of hardy functions into square integrable wavelets of constant shape, *SIAM J. Math. Anal.*, 15, 723-736.
- Haralick, R.M., 1984, Digital step edges from zero crossing of second directional filters, *IEEE Trans. Pattern Analy. Machine Intell.*, 6, 58-68.
- Harris, J., 1984, Lineament mapping of central Nova Scotia using Landsat-MSS and Seasat-SAR imagery, *Proc. 9th Canadian Symp. Remote Sens.*, St.John's, 359-373.
- Kaneko, T., 1978, Color composite pictures from principal axis components of multispectral scanner data, *IBM J. Res. Develop.*, 22, 386-392.
- Lowman, P.D. Jr., Harris, J., Masuoka, P.M., Singhroy, V.H., and Slaney, V.R., 1987, Shuttle imaging radar (SIR-B) investigations of the Canadian Shield; initial report, *IEEE Trans. Geosci., Remote Sensing.*, 25, 55-65.
- Mallat, S.G., 1989, A theory for multi-resolution signal decomposition: the wavelet representation, *IEEE Trans. Acoust. Speech, Signal Process.*, 11, 674-693.
- Masuoka, P.M., Harris, J., Lowman, P.D. Jr., and Blodget, H.W., 1987, Digital processing of orbital radar data to enhance geologic structure: examples from the Canadian Shield, *Photogramm. Eng. Remote Sens.*, 54, 621-632.
- Meyer, Y., 1986, Ondelettes, fonction splines, et analyses grauee, Univ. of Torino.
- Miao, X.G., and Moon, W.M., 1993, Application of wavelet transform in seismic data analysis, *Geophysics*, 58, (submitted).
- Moon, W.M., Won, J.S., Li, B., Slaney, V.R., and Lamontagne, M., 1991, Application of airborne C-SAR and SPOT image data to the geological setting of the Nahanni earthquake area, *Canadian J. Remote Sens.*, 17, 272-278.

- Morlet, J., Arenes, G., Fourgeau, E., and Giard, D., 1982. Wave propagation and sampling theory, *Geophysics*, 47, 203-236.
- Singhroy, V., 1992, Radar geology : Techniques and results, *Episodes*, 15, 15-20.
- Singhroy, V., Lowman, P.D., and Morasse, C.R., 1993. Analysis of ERS-1 SAR for Structural and Surficial Mapping in the Sudbury Basin, Canada, *Proceedings, Canadian Remote Sensing Symposium, Shebrook* (6pp).
- Won, J.S., 1993. Inversion of synthetic aperture radar (SAR) data using Born approximation, Ph.D. thesis, The University of Manitoba, Winnipeg, Canada.